GEOMETRIC STEREO CAMERA CALIBRATION WITH DIFFRACTIVE OPTICAL ELEMENTS

Denis Grießbach[*], Martin Bauer[*], Martin Scheele[*], Andreas Hermerschmidt[†], Sven Krüger[†]

[*] German Aerospace Center (DLR)
Institute of Robotics and Mechatronics
Rutherfordstrasse 2, 12489 Berlin, Germany
denis.griessbach@dlr.de

[†] HOLOEYE Photonics AG
Albert-Einstein-Str. 14, 12489 Berlin, Germany

Commission I/5

KEY WORDS: Geometric camera calibration, Stereo camera, Computer vision

ABSTRACT:

In order to use stereo camera based measurements in machine vision high accuracy geometric camera calibration is absolutely essential. For many applications, e.g. in optical navigation it is necessary to use the epipolar constraint to improve matching algorithms in terms of speed and reliability. Another field of application is the computation of high dense disparity maps where a precise image rectification is needed. The objective is to determine the interior camera parameters including a distortion model as well as the exterior orientation. Therefore, we introduce a two-step approach to calibrate a stereo camera system by means of diffractive optical elements. Working as a beam splitter with precisely defined diffraction angles, it produces a well known diffraction point pattern. As the virtual sources of the diffracted beams are points at infinity, the object to be imaged is invariant against translation. This particular feature allows a complete camera calibration with a single image avoiding complex bundle adjustments, resulting in a very fast and reliable single camera calibration. This procedure has been extended for stereo systems to determine the exterior orientation of both cameras. A comparison with classical photogrammetric methods using chessboard pattern and a calibration with fixed stars exploiting their accurate angular positions will show the capability of the introduced calibration method. The compact calibration setup also allows an in-field calibration.

1 INTRODUCTION

In order to use camera based measurements in machine vision high accuracy geometric camera calibration is absolutely essential. The objective is to determine the interior camera parameters needed for mapping 3D world coordinates to 2D image coordinates. For any application using stereo or even multi-camera images an exact knowledge about the exterior camera calibration is crucial. It is used to apply the epipolar constraint or to rectify images for calculating high dense disparity maps.

A common approach is the photogrammetric calibration using predefined calibration grids (Brown, 1971, Tsai, 1987). Several observations with different orientations are needed to estimate the camera parameters by minimizing a nonlinear error function. Due to a restricted grid size this technique is more or less limited to close range camera calibration. Another method eligible for far field camera calibration uses collimator-goniometer arrangements to illuminate a set of single pixels ($n \times m$). Knowing the directions of the collimated light, it is possible to estimate the camera parameters (Schuster and Braunecker, 2000). This fact is also used with stellar calibration using fixed stars with well known angular positions. A more comprehensive summary of key developments in camera calibration is provided in (Clarke and Fryer, 1998).

The calibration procedure reported here combines the particular advantages of calibration grid arrangements and single pixel illumination (Grießbach et al., 2008). By using diffractive optical elements (DOE) as beam splitters only one image with $n \times m$ diffraction points is needed to estimate the interior camera parameters. An extended procedure is proposed here to calibrate a stereo or multi-camera system. This method will be compared with a stellar calibration which is in fact working quite similar to the DOE calibration and a well optimized photogrammetric approach (Strobl et al., 2005) as a reference.

2 CAMERA CALIBRATION WITH DIFFRACTIVE OPTICAL ELEMENTS

DOEs can be used to split an incoming laser beam with wavelength λ into a number of beams with well-known propagation directions. As the image on the sensor is a Fraunhofer diffraction pattern, each projected image point represents a point at infinity, denoted in 3D projective space $\mathbb{P}^3$ by the homogeneous coordinate $\tilde{\mathbf{M}} = \left[X, Y, Z, 0\right]^T$ with,

$$\tilde{\mathbf{M}} = \begin{bmatrix} \lambda f_x \\ \lambda f_y \\ \sqrt{1 - \lambda^2 (f_x^2 + f_y^2)} \\ 0 \end{bmatrix} \tag{1}$$

where f_x, f_y denote a spatial frequency encoded in the DOE. With suitable computational algorithms (Hermerschmidt et al., 2007) it is possible to encode spatially aperiodic DOEs with arbitrary spatial frequencies, choosing the propagation directions freely. As they are easier to design for the large aperture diameters needed spatially periodic DOEs were used here. Their spatial frequencies are given by $f_{x,y} = n_{x,y}/g_{x,y}$, with n_x, n_y denoting the particular diffraction orders and grating constants g_x, g_y. The grating vectors are defining the $x-$ and $y-$axis of the DOE coordinate frame.

However, equation (1) is only valid if the incident light wave is a plane wave with uniform intensity distribution, perfectly perpen-

dicular to the DOE surface. In a real setup, the beam is finite in extension and often has a non-uniform intensity profile, which is typically Gaussian. Moreover, a slight tilt of the DOE with respect to the incident beam is hard to avoid.
The deviations of the real beam profile from a plane wave cause the diffraction spots in the far field to have a certain size, which can be estimated from the Convolution theorem of Fourier Optics (Goodman, 2004). For a more detailed analysis, a laser beam can be expressed by its angular spectrum. The consequent propagation directions are determined with the diffraction formula for non-perpendicular incidence to the DOE, which needs to be applied in our analysis anyway because of the potentially unavoidable tilt of the DOE with respect to the incident laser beam. For the following analysis, the DOE coordinate system will be used, in which the incident beam is given by,

$$\mathbf{r} = \left[\sin(\beta), -\sin(\alpha)\cos(\beta), \cos(\alpha)\cos(\beta)\right]^T \tag{2}$$

with the euler angles α and β rotating the $x-$ and $y-$axes of the DOE coordinate frame in terms of the collimator coordinate frame. The directions of the diffracted beams are now obtained as follows (R.C.McPhedran and L.C.Brown, 1980).

$$\tilde{\mathbf{M}} = \begin{bmatrix} \lambda f_x + r_x \\ \lambda f_y + r_y \\ \sqrt{1-(\lambda f_x + r_x)^2 - (\lambda f_y + r_y)^2} \\ 0 \end{bmatrix} \tag{3}$$

It is straightforward to calculate the diffracted beam directions in the DOE coordinate frame by simple matrix operations, therefore the somewhat lengthy expressions that are obtained as a result will be omitted. In order to transform the beam directions into the camera coordinate frame, the exterior orientation of the camera in terms of the DOE coordinate frame has to be considered,

$$\tilde{\mathbf{M}}' = \begin{bmatrix} \mathrm{R} & \mathbf{t} \\ 0 & 1 \end{bmatrix} \tilde{\mathbf{M}} \tag{4}$$

where R is a 3×3 rotation matrix defining the camera orientation and $\mathbf{t}$ the translation vector for the camera position. Equation (4) shows that the mapping of ideal points at infinity is invariant against translation which is a necessary condition for the following steps. This is also a great advantage compared to classical calibration grids for just one image is sufficient for calibration and therefore less parameters have to be estimated.

The accuracy of the diffraction angles depends on the accuracy both of the wavelength and the grating constants, as can be seen from equation (1). Therefore, gas lasers emitting precisely given wavelengths in the visible were used, rather than diode lasers which can easily drift in wavelength. The angular accuracy was checked with a collimator-goniometer arrangement finding only minor deviations from the computed values of less than $0.001°$.

Grating period	41.1 μm $\times$ 41.1 μm
Element diameter	75 mm
Angular spacing	$0.88°$
Highest diffraction order	[35, 35]
Max. diffraction angle	$\pm$ 46.1°

Table 1: DOE parameter for $\lambda = 632.8$ nm

2.1 Camera model

In projective space $\mathbb{P}$ mapping of a homogeneous object point $\tilde{\mathbf{M}} \in \mathbb{P}^3$ to an image point $\tilde{\mathbf{m}} \in \mathbb{P}^2$ is defined with,

$$\tilde{\mathbf{m}} = \mathrm{P}\tilde{\mathbf{M}} \tag{5}$$

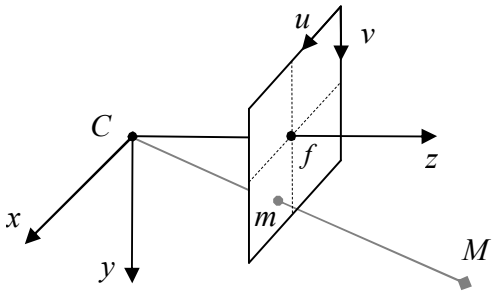

Figure 1: Pinhole camera model

where P is a 3×4-projection matrix consisting of the parameters of the interior- and exterior orientation of the camera.

$$\mathrm{P} = \mathrm{K}\left[\mathrm{R}|\mathbf{t}\right] \tag{6}$$

with $\mathrm{R}, \mathbf{t}$ describing the rotational matrix and translation of the exterior orientation and the camera matrix K containing the focal length f and the principal point $\left[u_0, v_0\right]^T$.

$$\mathrm{K} = \begin{bmatrix} f & 0 & u_0 \\ 0 & f & v_0 \\ 0 & 0 & 1 \end{bmatrix} \tag{7}$$

The ideal beam direction $\mathbf{M}' = \left[X', Y', Z'\right]^T$ denoted in euclidean representation $\mathbb{R}^3$ is mapped into 2D image coordinates by projecting it on the plane $Z' = 1$

$$\begin{bmatrix} x \\ y \\ 1 \end{bmatrix} = \begin{bmatrix} X'/Z' \\ Y'/Z' \\ 1 \end{bmatrix} \tag{8}$$

with x, y representing the ideal normalized image coordinates. From equation (5, 6) we get the ideal pixel image coordinates $\tilde{\mathbf{m}} = [u, v, 1]^T$.

$$\begin{bmatrix} u \\ v \\ 1 \end{bmatrix} = \mathrm{K}\begin{bmatrix} x \\ y \\ 1 \end{bmatrix} \tag{9}$$

Before applying the pinhole model lens distortion has to be considered. There are several distortion models available. The most common is the radial distortion model by Brown (Brown, 1971) considering pincushion or barrel distortion which is expressed as follows,

$$\begin{bmatrix} \hat{x} \\ \hat{y} \end{bmatrix} = \begin{bmatrix} x \\ y \end{bmatrix}\left(1 + k_1 r^2 + k_2 r^4 + k_3 r^6 + \cdots\right) \tag{10}$$

with

$$r^2 = x^2 + y^2 \tag{11}$$

The complete mapping of ideal points to distorted image coordinates $\left[\hat{u}, \hat{v}\right]^T$ is subsumed to

$$\begin{bmatrix} x \\ y \end{bmatrix} \mapsto \begin{bmatrix} \hat{u} \\ \hat{v} \end{bmatrix} = \begin{bmatrix} u_0 \\ v_0 \end{bmatrix} + f\begin{bmatrix} x \\ y \end{bmatrix}\left(1 + k_1 r^2 + k_2 r^4 + k_3 r^6 + \cdots\right) \tag{12}$$

Given a set of correspondent points $\tilde{\mathbf{M}} \leftrightarrow \left[\hat{u}, \hat{v}\right]^T$ we seek to minimize the cost function

$$\min_m \left\| \begin{bmatrix} \hat{u} - u_0 \\ \hat{v} - v_0 \end{bmatrix} - f\begin{bmatrix} x \\ y \end{bmatrix}\left(1 + k_1 r^2 + k_2 r^4 + k_3 r^6 + \cdots\right) \right\|^2 \tag{13}$$

where $m = \left[f, u_0, v_0, k1, k2, k3, \omega, \varphi, \kappa, \alpha, \beta\right]^T$ describing the interior and exterior orientation of the camera and a possible ro-

tation (α, β) of the DOE in terms of the collimation coordinate frame. For the mapping to be invariant against translation the exterior orientation only consists of the rotation matrix R which is expressed by the euler angles ω, φ, κ. Correspondent points are found by an iterative approach constantly refining the model parameters. The result is improved by calculating the centroids of the diffraction points which gives subpixel accuracy.

2.2 Single camera calibration setup

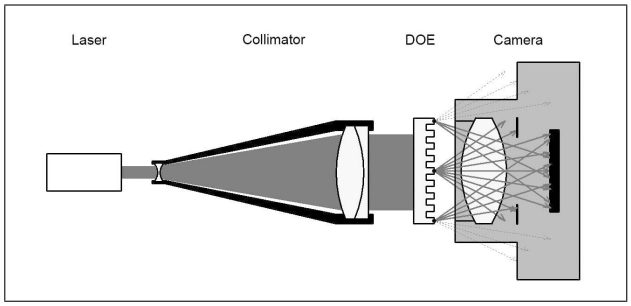

Figure 2: Scheme of camera calibration with DOE

The principle scheme for geometrical sensor calibration is illustrated in figure 2. A helium-neon laser with a wavelength of 632.8 nm is collimated and enlarged with a beam expander to a diameter of 78 mm. The enlarged beam is then diffracted by a DOE which is located directly in front of the camera optics. The diameter of the incident laser beam and that of the DOE active area should at least as large as the aperture diameter of the camera lens. Each of the diffracted beams is focused within the image plane of the camera. In order to obtain spots covering the whole sensor area, the maximum diffraction angle of the DOE should be larger than the field of view of the camera. No further alignment steps are necessary, because firstly the mapping of the diffraction points is invariant against translation, and secondly the rotation of the DOE in terms of the collimation system as well as the exterior orientation of the camera is modeled and can thus be determined (Grießbach et al., 2008).

2.3 Multi camera calibration

Many applications in computer vision require two or more cameras. To apply epipolar geometry which is important for finding correspondences in multiple views a very good knowledge about their relative exterior orientation is needed. As a by-product from single camera calibration the rotation $\mathrm{R}(\omega, \varphi, \kappa)$ from DOE coordinate frame to camera coordinate frame is determined. In case the base distance between the cameras of a stereo system is small, illuminating both cameras at ones it is evident that the relative rotation $\Delta\mathrm{R}$ between both camera frames is,

$$\Delta\mathrm{R} = \mathrm{R}_2 \cdot (\mathrm{R}_1)^{-1} \tag{14}$$

But more likely is a larger base distance allowing only for single camera illumination. Therefore, after having the first camera calibrated either the camera system or the calibration setup is shifted until the second camera is seeing the diffracted beams. Doing this by pure translation still allows to apply equation (14).
Since the mapping is invariant against translation it can not be determined with this setup. For this reason a scale, e.g. a calibration grid is used for estimating the base distance. The advantage over classical methods is that the parameters of interior orientation and relative rotation are already determined independently for each camera and only the translation has to be estimated. Of course, it would be possible to estimate the full relative exterior orientation including rotation but this leads to bigger errors as rotation and translation are not fully independent.

3 STELLAR CALIBRATION

Fixed star angular position are recorded and used for different purposes, e.g. navigation or time measurement over a long time. Nowadays these positions are very well known due to satellite measurements. The Hipparcos star catalog will be used here (The Hipparcos and Tycho Catalogues, 1997).
Calibrating a camera system with stars is in fact quite similar with the proposed DOE calibration method. First an image of the starry sky has been made and the seen stars were associated with their precise position (directions) from the catalog. Additionally the atmospheric refraction which causes astronomical objects appear higher in the sky as they are has to be taken into account. It is zero in the zenith but more than 1 pixel ($\approx 0.1^\circ$) at 10°over the horizon and therefore a source of error. An approximation is shown in the following equation,

$$\Delta h = (60\tan(h) - 0.06\tan(h)^3)/3600 \tag{15}$$

where h denotes the zenith distance of an object. To apply this formula the angular position given in equatorial coordinates in the star catalog has to be transformed into the horizontal coordinate frame. Therefore the exact position and time of the star image is needed.

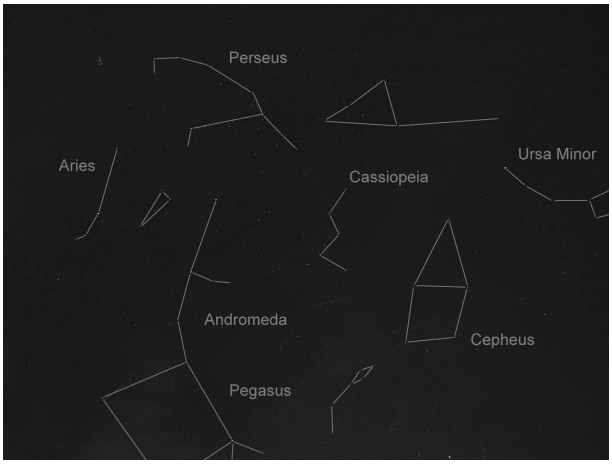

Figure 3: Star image (enhanced, constellations added)

Again as in DOE calibration the rotation from camera coordinate frame to a reference frame (horizontal system) is determined. Doing this for both cameras of the stereo system enables to determine the relative rotation of the cameras with equation (14).

4 RESULTS

To prove the validity of the proposed method a stereo camera system with 200 mm base distance has been calibrated with the DOE setup, a stellar calibration using fixed star positions and a classical photogrammetric chessboard pattern calibration (Strobl et al., 2005).

Prosilica GC 1380H	
Sensor size	1360×1024
Pixel size	6.45 μm
Focal length	4.8 mm
iFoV	0.077 deg
FoV	42.8×34.5 deg

Table 2: Camera parameters

4.1 Interior Orientation

The photogrammetric chessboard pattern calibration was achieved with an elaborate method using 10 differnt poses with additional external pose measurements. The parameters of interior and exterior orientation are estimated in a complex bundle adjustment. This is a major difference to the DOE and stellar calibration were the interior parameters are determined independently for each camera with a single image. Table 3 and 4 are showing the results with f, u_0, v_0 are stated in pixel values. The distortion parameters are without dimension but applying to normalized image coordinates as seen in equation (10). σ denotes the residual error in pixel values obtained with n measurements.

	DOE	Stars	Chessboard
f	773.6	772.5	772.4
u_0	655.2	653.4	655.2
v_0	545.3	545.2	546.3
k_1	-0.25697	-0.25026	-0.24691
k_2	0.10988	0.10198	0.09891
k_3	-0.02440	-0.02128	-0.02020
n	7119	367	1436
σ	0.12	0.18	0.21

Table 3: Interior parameters for left camera

	DOE	Stars	Chessboard
f	771.4	770.0	770.3
u_0	709.9	709.8	709.1
v_0	503.9	503.8	504.5
k_1	-0.25686	-0.24733	-0.24799
k_2	0.11071	0.09548	0.10055
k_3	-0.02494	-0.01793	-0.02073
n	7324	383	1445
σ	0.12	0.17	0.21

Table 4: Interior parameters for right camera

It can be seen that despite of the very different methods the results are quite comparable with a slightly better residual error for the DOE measurement. Figure 4 shows the equally distributed diffraction points covering the whole image which also applies for the star calibration (figure 5). This is not the case for the photogrammetric calibration where border areas of the image are often without measurement points which is a disadvantage for calculating the distortion model. Both figures also show the random character of the error vectors which are enlarged for visibility.

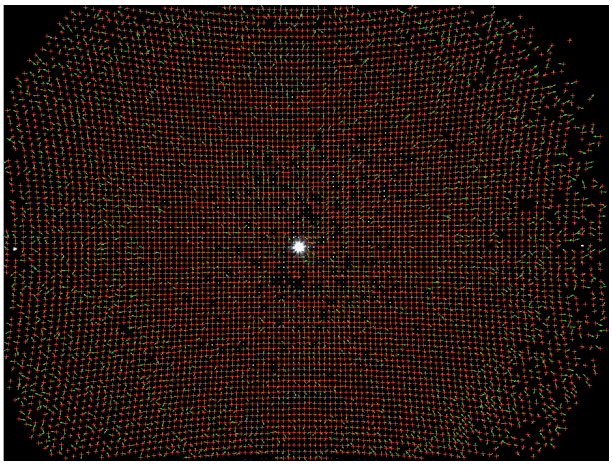

Figure 4: DOE image with associated points including enlarged residual errors

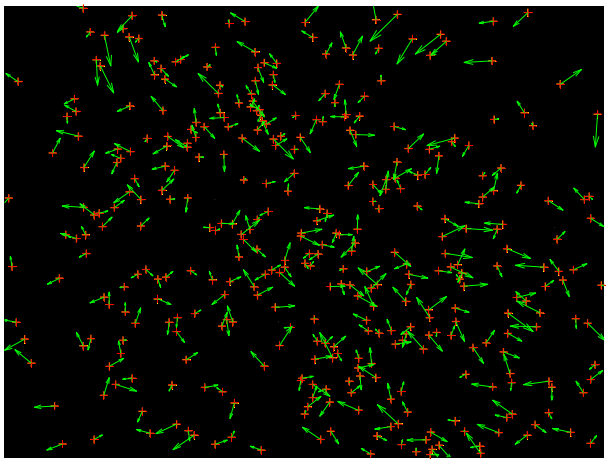

Figure 5: Star image with associated stars including enlarged residual errors

Figure 6 shows the strong distortion of the used 4.8 mm lens with a displacement of more than 100 pixel in the outer regions of the image. For a better visibility only every second diffraction point is displayed here. The used distortion model was just adequate in this case. A correction for radial distortion is shown in Figure 7 and 8.

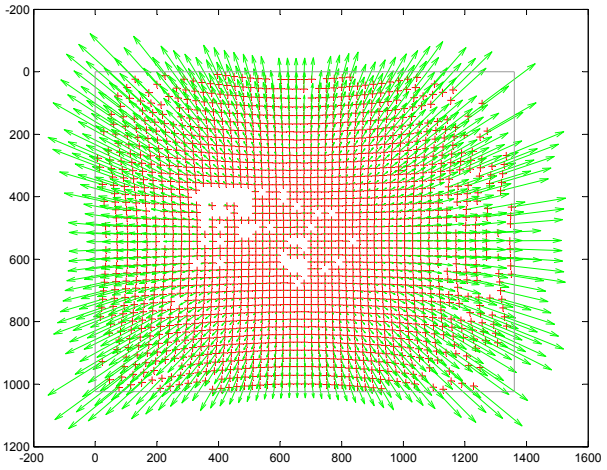

Figure 6: DOE image with reduced point field and radial distortion vectors

4.2 Exterior Orientation

In the photogrammetric approach the relative exterior orientation is estimated directly within the complex bundle adjustment. It was assumed that the relative orientation of both cameras is fixed for all 10 poses. Since with DOE and stars the mapping from points at infinity is invariant against translation only the rotation is estimated separately for each camera as by-product from interior calibration and used as shown in section 2.3. One stereo image from the photogrammetric calibration is now taken to determine the translational parameters with knowledge of the interior orientation and relative rotational parameters.
Again the achieved parameters are alike, though with a small advantage for the DOE and stellar calibration as seen with the interior orientation (Table 5). The exterior parameters are stated in degree and mm whereas the residual error σ is given in pixel values.

	DOE	Stars	Chessboard
ω	0.103	0.077	0.118
φ	-0.654	-0.654	-0.568
κ	0.311	0.289	0.362
t_x	-200.0	-200.0	-200.2
t_y	-1.1	-1.2	-0.6
t_z	-1.2	-1.2	-1.3
n	314	314	2881
σ	0.14	0.17	0.77

Table 5: Exterior orientation of the stereo system

5 CONCLUSION

A method for single geometrical camera calibration including an extension for multi camera systems was proposed. It uses custom-made diffractive optical elements working as beam splitters with precisely known diffraction angles. As the virtual sources of the diffracted beams are points at infinity, the object to be imaged is similar to the starry sky, which gives a image invariant against translation. This particular feature allows a complete camera calibration with a single image avoiding complex bundle adjustments, resulting in a very fast, easy to use and reliable calibration procedure. The method was shown on an wide-angle lens but also applies for far field calibration with telephoto lenses which is difficult to manage with classical methods.

The achieved results are in accordance with classical camera calibration using the pinhole camera model and a radial distortion model. This is proved by comparing results from DOE, stellar and photogrammetric calibration noticing a slight advantage for the DOE concept. Stellar calibration is also working very well but difficult to handle due to dependencies regarding weather, light pollution and various influences of the atmosphere.

Furthermore, the approach has been extended for multi camera systems where the determination of the relative exterior orientation is essential. Due to a translational invariant mapping an additional stereo image of a calibration chart is needed to achieve a complete exterior orientation including translational parameters.

It is to stress that the results from the photogrammetric calibration are accomplished only with a complex arrangement to support the estimation with external pose measurements. This means an improvement compared with commonly used methods regarding accuracy and repeatability. The achieved results are also depended on the used poses which means an additional error source if not conducted properly.

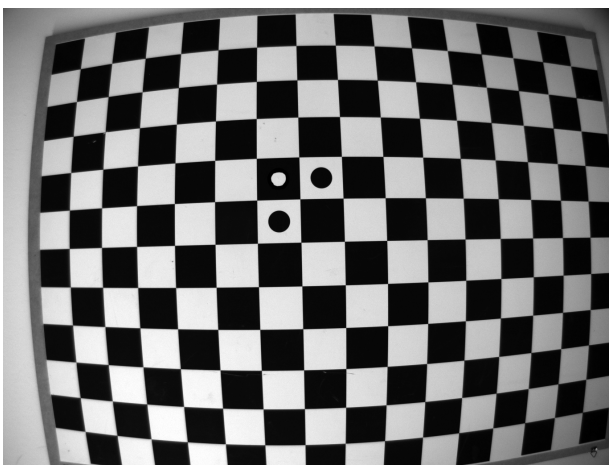

Figure 7: Original image

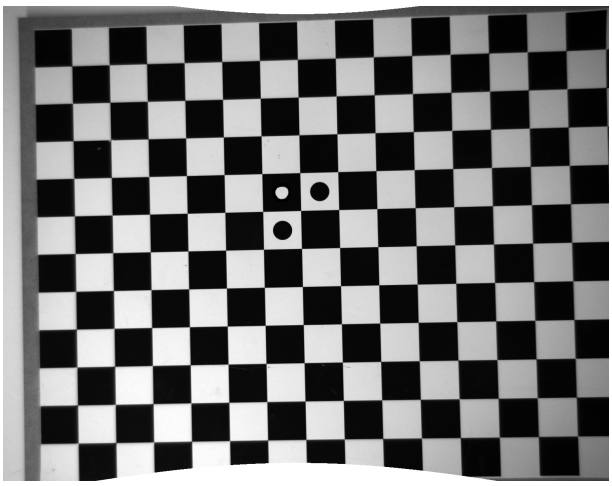

Figure 8: Corrected image

REFERENCES

Brown, D. C., 1971. Close-range camera calibration. Photogrammetric Engineering 37, pp. 855–866.

Clarke, T. A. and Fryer, J. G., 1998. The development of camera calibration methods and models. The Photogrammetric Record 16(91), pp. 51–66.

Goodman, J. W., 2004. Introduction to Fourier Optics. 3 edn, Roberts & Company Publishers.

Grießbach, D., Bauer, M., Hermerschmidt, A., Krüger, S., Scheele, M. and Schischmanow, A., 2008. Geometrical camera calibration with diffractive optical elements. Opt. Express 16(25), pp. 20241–20248.

Hermerschmidt, A., Krüger, S. and Wernicke, G., 2007. Binary diffractive beam splitters with arbitrary diffraction angles. Opt. Lett. 32(5), pp. 448–450.

The Hipparcos and Tycho Catalogues, 1997.

R.C.McPhedran, G. and L.C.Brown, 1980. Electromagnetic theory of gratings. Springer Verlag Berlin, chapter R.Petit (ed.), pp. 227–275.

Schuster, R. and Braunecker, B., 2000. The calibration of the adc (airborne digital camera) -system. Int. Arch. of Photogrammetry and Remote Sensing pp. 288–294.

Strobl, K. H., Sepp, W., Fuchs, S., Paredes, C. and Arbter, K., 2005. DLR CalLab and DLR CalDe.

Tsai, R., 1987. A versatile camera calibration technique for high-accuracy 3d machine vision metrology using off-the-shelf tv cameras and lenses. Robotics and Automation, IEEE Journal of 3(4), pp. 323–344.